

# Eutherian-Specific Gene *TRIML2* Attenuates Inflammation in the Evolution of Placentation

Xuzhe Zhang <sup>\*,1,2,3</sup> Mihaela Pavlicev,<sup>1,2,3</sup> Helen N. Jones,<sup>4,5</sup> and Louis J. Muglia<sup>\*,1,2,3</sup>

<sup>1</sup>Division of Human Genetics, Center for Prevention of Preterm Birth, Perinatal Institute, Cincinnati Children's Hospital Medical Center, Cincinnati, OH

<sup>2</sup>Department of Pediatrics, University of Cincinnati College of Medicine, Cincinnati, OH

<sup>3</sup>March of Dimes Prematurity Research Center Ohio Collaborative, Cincinnati, OH

<sup>4</sup>Division of Pediatric Surgery, Cincinnati Children's Hospital Medical Center, Cincinnati, OH

<sup>5</sup>Department of Surgery, University of Cincinnati College of Medicine, Cincinnati, OH

\*Corresponding authors: E-mails: xuzhe.zhang@cchmc.org; louis.muglia@cchmc.org.

Associate editor: Yoko Satta

## Abstract

Evolution of highly invasive placentation in the stem lineage of eutherians and subsequent extension of pregnancy set eutherians apart from other mammals, that is, marsupials with short-lived placentas, and oviparous monotremes. Recent studies suggest that eutherian implantation evolved from marsupial attachment reaction, an inflammatory process induced by the direct contact of fetal placenta with maternal endometrium after the breakdown of the shell coat, and shortly before the onset of parturition. Unique to eutherians, a dramatic downregulation of inflammation after implantation prevents the onset of premature parturition, and is critical for the maintenance of gestation. This downregulation likely involved evolutionary changes on maternal as well as fetal/placental side. *Tripartite-motif family-like2 (TRIML2)* only exists in eutherian genomes and shows preferential expression in preimplantation embryos, and trophoblast-derived structures, such as chorion and placental disc. Comparative genomic evidence supports that *TRIML2* originated from a gene duplication event in the stem lineage of Eutheria that also gave rise to eutherian *TRIML1*. Compared with *TRIML1*, *TRIML2* lost the catalytic RING domain of E3 ligase. However, only *TRIML2* is induced in human choriocarcinoma cell line JEG3 with poly(I:C) treatment to simulate inflammation during viral infection. Its knockdown increases the production of proinflammatory cytokines and reduces trophoblast survival during poly(I:C) stimulation, while its overexpression reduces proinflammatory cytokine production, supporting *TRIML2*'s role as a regulatory inhibitor of the inflammatory pathways in trophoblasts. *TRIML2*'s potential virus-interacting PRY/SPRY domain shows significant signature of selection, suggesting its contribution to the evolution of eutherian-specific inflammation regulation during placentation.

**Key words:** TRIM family protein, Eutheria, placentation, inflammation, endogenous retrovirus, coevolution.

## Introduction

Although both eutherians and marsupials are viviparous and form fully functional placentas during pregnancy, eutherian ancestors evolved highly invasive form of placentation, with subsequent extension of pregnancy. These reproductive characteristics enabled the offspring to be born at more mature stages and set eutherians apart from other mammals (Wildman et al. 2006; Renfree 2010; Chavan et al. 2016). Underlying such remarkable evolutionary achievement unique to eutherian reproduction is the mechanism that enables the semi-allogeneic fetus direct contact with, and breaching of the integrity of maternal tissue without the rejection by the maternal immune system (Chavan et al. 2017). Recent comparative studies in mammals with different reproduction modes have shed light on this conundrum (Griffith et al. 2017).

Though viviparous, marsupials retain many characteristics of the oviparous ancestors that are seen in extant monotremes. In both marsupials and monotremes, the contact

between the conceptus and maternal tissue is limited by a layer consisting of the zona pellucida, mucoid coat, and shell coat (Frankenberg and Renfree 2018). In monotremes, the shell coat thickens dramatically as pregnancy proceeds (Frankenberg 2018). In marsupials, instead of thickening, the shell coat breaks down and enables transient direct attachment of the placenta to the endometrium, which triggers maternal inflammation reaction and results in parturition within days. Interestingly, implantation processes in eutherians show molecular signatures consistent with the marsupial attachment reaction, but unlike marsupials, the upregulation of proinflammatory genes does not trigger parturition. Rather, a transition into an anti-inflammatory period occurs, and the low inflammatory status is maintained until the end of the extended pregnancy (Griffith et al. 2017).

The preservation and modification of the inflammatory reaction associated with implantation throughout evolution suggest that it is a critical process. Indeed, evidence supports that inflammation is constitutive for the establishment of

© The Author(s) 2019. Published by Oxford University Press on behalf of the Society for Molecular Biology and Evolution.

This is an Open Access article distributed under the terms of the Creative Commons Attribution License (<http://creativecommons.org/licenses/by/4.0/>), which permits unrestricted reuse, distribution, and reproduction in any medium, provided the original work is properly cited.

Open Access

pregnancy, due to its pregnancy-enhancing aspects in processes such as angiogenesis (Chaouat 2013). On the other hand, excessive inflammation, on maternal and/or fetal/placental sides, is associated with adverse reproductive outcomes, such as fetal loss (Zenclussen et al. 2003; Calleja-Agius et al. 2012). Thus, the evolution in eutherians of mechanisms to tightly control the nature and extent of inflammation both temporally and spatially was crucial to enable the transition to the anti-inflammatory status unique to eutherian prolonged pregnancies.

Maternal-fetal tolerance is not the only source of selective pressure on the eutherian immune regulation during pregnancy. Other important sources are infectious pathogens. Intrauterine infection lowers maternal reproductive fitness (Mor 2008). Expansion of gene families involved in immune response often accompanies such arms races between hosts and pathogens (Worobey et al. 2007). One gene family that shows such rapid expansion is the tripartite motif (TRIM) family, thus named due to the N-terminal RBCC (RING, B-box, and coiled-coil) motif (Cao et al. 1997). Although each of these three submotifs also exists independently in plants, the order of combination is conserved since early in metazoan evolution. Afterward, the RBCC domain has been associated with several different C-terminal domains; however, the RBCC domain per se has been evolving as a single block without domain-swapping between TRIMs. There is no evidence for domain acquisition in RBCC motif, however domain loss that results in the lack of at least one of the three N-terminal domains has happened multiple times, and has given rise to the noncanonical TRIM-like members of this protein family. Based on their protein structure and evolutionary history, TRIMs can be divided into two groups. Group-1 TRIMs possess a variety of C-terminal motifs and are shared by invertebrates and vertebrates, and group-2 TRIMs use SPRY domain as the core C-terminal motif and can only be found in vertebrate genomes. The association of N-terminal RBCC with C-terminal SPRY domain is followed by rapid evolution and gene expansion through gene duplication in vertebrate genomes (Sardiello et al. 2008). The first major expansion of group-2 TRIMs co-occurred with the evolution of the adaptive immunity in jawed vertebrates. Subsequent expansions often paralleled major developments of the immune system, especially the evolution of an ever more complex interferon pathway (Versteeg et al. 2014). Functionally, many TRIMs can be induced by the activation of pattern-recognition receptors during infection, and through their E3 ligase activity, regulate the production of proinflammatory cytokines, thus influence the course of inflammation and innate immunity (Ozato et al. 2008). Through gene duplication, the TRIM family can function as a reservoir to provide new TRIM genes to fine-tune the inflammation/immune response.

As the TRIM family shows rapid expansion in eutherian genomes, we hypothesized that some of these eutherian-specific TRIMs, especially those with preferential expression at the maternal-fetal interface, may contribute to the establishment of the eutherian-specific anti-inflammatory phase. To test this hypothesis, we carried out comparative genomic

studies and gene expression profiling, and found that *tripartite-motif family-like 2* (*TRIML2*) only exists in eutherian genomes and is expressed preferentially in preimplantation embryos, chorion, and placental disc. Functional study in human choriocarcinoma cell line JEG3 supports that *TRIML2* reduces proinflammatory cytokine production in trophoblasts. Multiple sites of *TRIML2* PRY/SPRY domain, which have been demonstrated to contribute to retrovirus restriction function of other TRIMs, show significant signature of positive selection, supporting the notion that *TRIML2* may have contributed to the evolution of inflammation regulation during eutherian placentation.

## Results

### *TRIML2* Exists in All Extant Eutherian Superorders but Is Absent in Marsupial and Monotreme Genomes

To study the role TRIMs played during the evolution of eutherian placentation, we looked for TRIMs that likely evolved in the stem lineage of eutherians, that is, after the separation of marsupials but before the branching of the four extant eutherian superorders. As many TRIMs, especially vertebrate-specific group-2 TRIMs, exist in spatial gene clusters (Versteeg et al. 2014), we scanned for TRIM clusters that exist in all four representative species of extant eutherian superorders through UCSC genome browser, and found that *TRIML1* and *TRIML2* at the telomeric end of the long arm of human chromosome 4 exist in all four representative species (fig. 1A–C). We downloaded protein sequences of *TRIML1* and *TRIML2* of all eutherians with well-documented placentation interdigitation and invasiveness (56 species, supplementary fig. S1, Supplementary Material online), and verified through BLAST that *TRIML1* proteins of any two eutherian species always find each other as the best hit in the opposite genome with e-value 0.0. Similarly, eutherian *TRIML2* proteins also meet the Reciprocal Best Hits (RBH) criterion for ortholog detection (Moreno-Hagelsieb and Latimer 2008). This evidence supports the existence of *TRIML1* and *TRIML2* orthologs in all four extant eutherian superorders, which suggests that both genes evolved before the separation of the four extant eutherian superorders.

To help estimate the gene age of *TRIML1* and *TRIML2*, we used human *TRIML1* and *TRIML2* as queries and performed Blastp searches against nonredundant protein sequence databases of taxa Reptilia, Monotremata, and Marsupialia. In reptilian genomes, no genes are annotated as *TRIML1*, and the most similar genes of both human *TRIML1* and *TRIML2* are TRIM39-like proteins. However, reptilian TRIM39-like proteins show highest similarity with eutherian TRIM39 in the reciprocal search rather than eutherian *TRIML1* or *TRIML2*, supporting the lack of orthologs of either *TRIML1* or *TRIML2* in Reptilia.

In monotreme and marsupial genomes, the proteins most similar to human *TRIML1* and *TRIML2* are both protein products of genes annotated as probable *TRIML1*. However, unlike eutherian genomes, which have exactly one gene annotated as *TRIML1* per species, multiple probable *TRIML1* genes are annotated in each of the four available marsupial

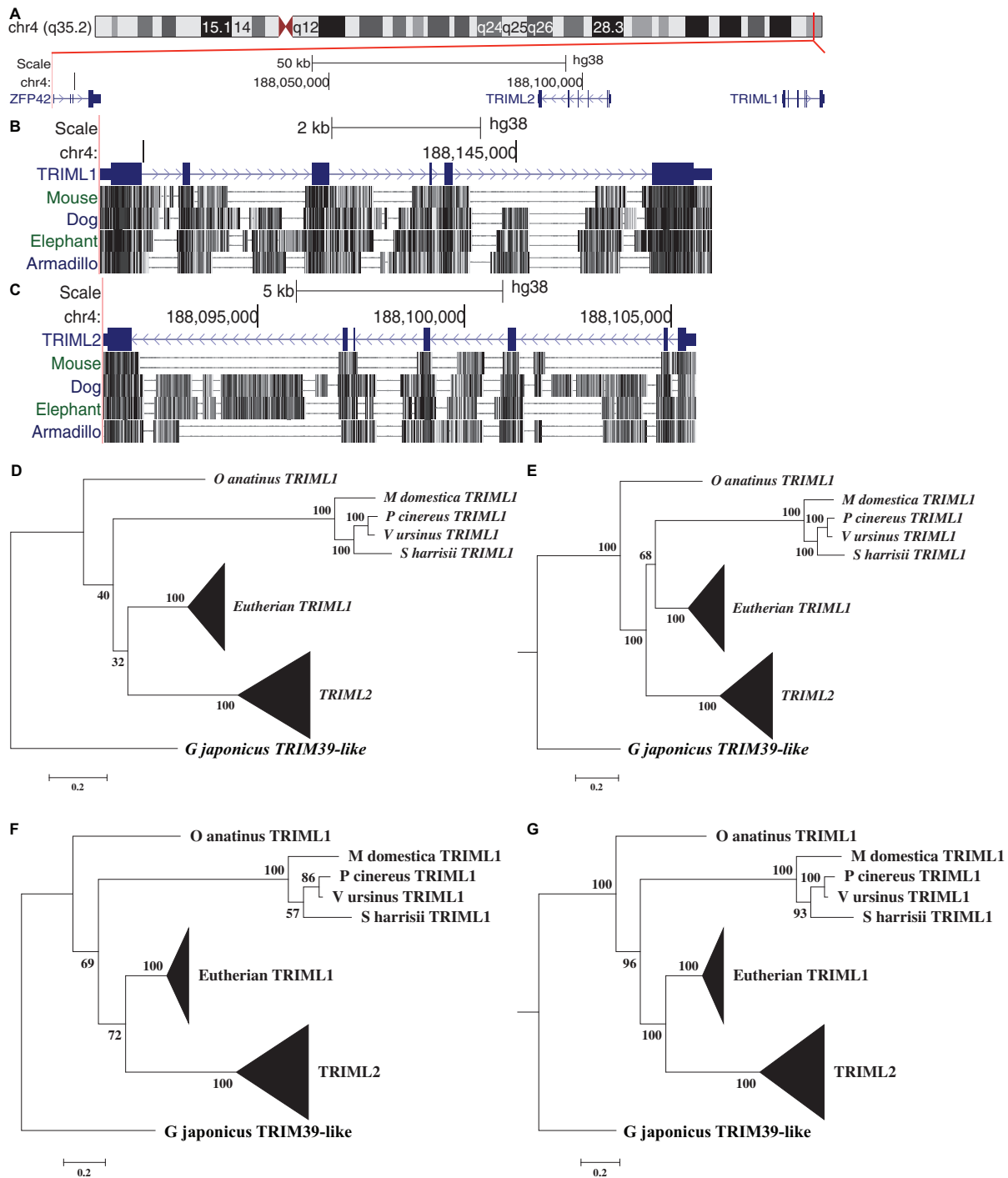


**FIG. 1.** *TRIML2* likely resulted from a gene duplication event in eutherian stem lineage. (A) Human *TRIML1* and *TRIML2* are located at the telomeric end of the long arm of chromosome 4. (B and C) Multiple alignments of *TRIML1* and *TRIML2* loci show both genes exist in all four superorders of eutherian. (D–G) Phylogenetic trees generated through maximum likelihood (D, mRNA tree; F, protein tree) and Bayesian analyses (E, mRNA tree; G, protein tree), with bootstrap percentages/posterior probabilities.

genomes and the monotreme platypus genome. This result is possibly due to genome assembly limitations and gene annotation errors intrinsic to draft genome assemblies (Denton et al. 2014) and exacerbated by the similarities between members of the large *TRIM* family that complicate the differentiation between orthologs and paralogs (Tekai 2016). We have used RNA-seq data to complement gene annotation information, knowing that human *TRIML1* and *TRIML2* show

restricted tissue distribution that is biased toward testis and placenta (fig. 2, see next section for detailed verification). As in the platypus genome only one of the annotated *TRIML1* transcripts (XM\_007670587) appears restricted in expression in ovary and low-level expression in testis (GSE43520, Necsculea et al. 2014; GSE97367, Marin et al. 2017), assuming that the expression pattern of *TRIML1* gene is somewhat conserved, we suggest that this sequence is the ortholog of

eutherian *TRIML1*. Of the four marsupial species with genomes curated by NCBI, the gray short-tailed opossum is the best studied. Two probable *TRIML1* gene transcripts (XM\_007491153 and XM\_016422056) are supported by RNA-seq data with restricted expression in testis and ovary (GSE43520, Neacsulea et al. 2014; GSE97367, Marin et al. 2017; GSE106077, Chen et al. 2019) and low-level expression in placenta (GSE45211, Wang et al. 2014; GSE79121, Armstrong et al. 2017). Using the corresponding protein sequences as queries to search against the other three marsupial protein databases, we found high-level homology (bit-score >500, e-value 0.0) to exactly one probable *TRIML1* protein per species (*Vombatus ursinus* XP\_027712198, *Phascolarctos cinereus* XP\_020831575, and *Sarcophilus harrisii* XP\_012400891). Interestingly, of all potential marsupial *TRIML1* proteins, only these three *TRIML1* proteins and the opossum *TRIML1* XP\_007491215 (protein product of XM\_007491153) meet the Reciprocal Best Hits criterion with each other, supporting the idea that they form a single marsupial ortholog group. As three of the four marsupial genomes have only one copy of this gene, and genome fragmentation during sequencing tends to falsely increase predicted gene numbers (Denton et al. 2014), the two highly similar opossum *TRIML1* genes (82% identical for mRNA and 71% identical for protein) located in tandem are more likely to be genome assembly and annotation artifacts, although it cannot be ruled out that a unique gene duplication event happened in opossum lineage. We constructed phylogenetic trees of *TRIML1* and *TRIML2* based on mRNA and protein sequences, using *Gekko japonicus TRIM39-like*, the reptilian *TRIM* that shows the highest homology to both *TRIML1* and *TRIML2*, as outgroup. Using both *G. japonicus TRIM39-like* and mammalian *TRIM39* sequences as outgroups does not change the topology of the part of the phylogenetic tree concerning the evolutionary relationship of *TRIML1* and *TRIML2*, thus supporting the choice of *TRIM39* as an outgroup (supplementary fig. S2, Supplementary Material online). Using both potential opossum *TRIML1* sequences or only one does not change the overall tree topology regarding eutherian *TRIML1*, marsupial *TRIML1* and *TRIML2* (fig. 1D–G and supplementary fig. S3, Supplementary Material online). Maximum likelihood trees based on mRNA (fig. 1D and supplementary fig. S3A and E, Supplementary Material online) and protein (fig. 1F and supplementary fig. S3C and G, Supplementary Material online) and Bayesian analyses based on protein (fig. 1G and supplementary fig. S3D and H, Supplementary Material online) support that *TRIML2* arose from a gene duplication event that occurred in stem eutherian lineage that also gave rise to eutherian *TRIML1*. However in these trees the alternative situation that *TRIML2* arose from a gene duplication event in the eutherian and marsupial common ancestor, followed by loss of *TRIML2* in marsupial lineage, as is supported by Bayesian analyses based on mRNA (fig. 1 and supplementary fig. S3B and F, Supplementary Material online), cannot be ruled out with the currently available information. Nevertheless, a comparison of protein structures reveals that monotreme, marsupial, and eutherian *TRIML1* all have the RING domain in the N-terminal motif,

while *TRIML2* lost this critical domain for E3 ligase function (fig. 5A). Thus the existence of the RING-less *TRIML2* is eutherian-specific either through eutherian-specific genetic innovation or through eutherian-specific gene fixation.

### *TRIML1* and *TRIML2* Expression Domains Are Restricted to Preimplantation Embryo, Trophoblast, Ovary, and Testis

To test the hypothesis that *TRIML1* and/or *TRIML2* have functions at the maternal-fetal interface, we first assessed their expression pattern using tissue-specific RNA-Seq data from the Human Protein Atlas (Fagerberg et al. 2014). Unlike most *TRIM* genes, which are broadly expressed (Ozato et al. 2008), most human tissues do not express *TRIML1* or *TRIML2*, except for testis and placenta (fig. 2A). *TRIM42* also exhibits testis-restricted expression, however, it is not expressed in human or mouse placenta (Fagerberg et al. 2014; Yue et al. 2014). It also lacks expression in human choriocarcinoma cell lines such as BeWo (Fagerberg et al. 2014), which does express both *TRIML1* and *TRIML2* (supplementary table S1, Supplementary Material online). Furthermore, *TRIM42* exists in reptile and bird genomes (data not shown), suggesting it is unlikely that its main role in eutherians would be in placenta.

We verified that *TRIML1* and *TRIML2* are expressed in human extraembryonic tissues at term by qPCR, and discovered that both of them show higher expression in the fetal membranes than in the placental disc, with *TRIML1* more abundant in amnion, a structure derived from the inner cell mass, and *TRIML2* more abundant in chorion, a structure with a large contribution from trophoblast (Luckett 1975; Pijnenborg et al. 1981) (one-way ANOVA, Tukey's HSD; amnion vs. chorion,  $P < 0.01$ ) (fig. 2B).

To gain detailed information on the expression pattern of *Triml1* and *Triml2* in tissues of earlier stages during eutherian pregnancy, we examined their mRNA levels by qPCR in mouse. Both genes are expressed in preimplantation embryos. However, as the embryo develops further, robust expression can no longer be detected in various fetal tissues, but is restricted to the extraembryonic structures. Despite the differences in extraembryonic structure development between mouse and human, mouse fetal membranes also show the highest expression level among extraembryonic structures, followed by the placental labyrinth, while junctional zone together with the decidua show more modest, yet robust expression (fig. 2C). RNAscope assays show similar expression patterns in these structures (fig. 2E). We tested expression at different time during pregnancy, and fetal membranes always show higher expression for both *Triml1* and *Triml2* than the labyrinth (*t*-test, *Triml1*:  $P < 0.01$  for at all time points, *Triml2*:  $P < 0.05$  for at all time points) (fig. 2D).

Mouse adult tissues confirm restricted expression patterns for both *Triml1* and *Triml2*. Although highest expression of *Triml1* is seen in adult testis, *Triml2* expression in adult tissues is lower than preimplantation embryos, placental labyrinth, and fetal membranes (fig. 2C). We investigated expression in the female reproductive systems in virgins and during pregnancy (E15.5); both *Triml1* and *Triml2* expression in ovary are

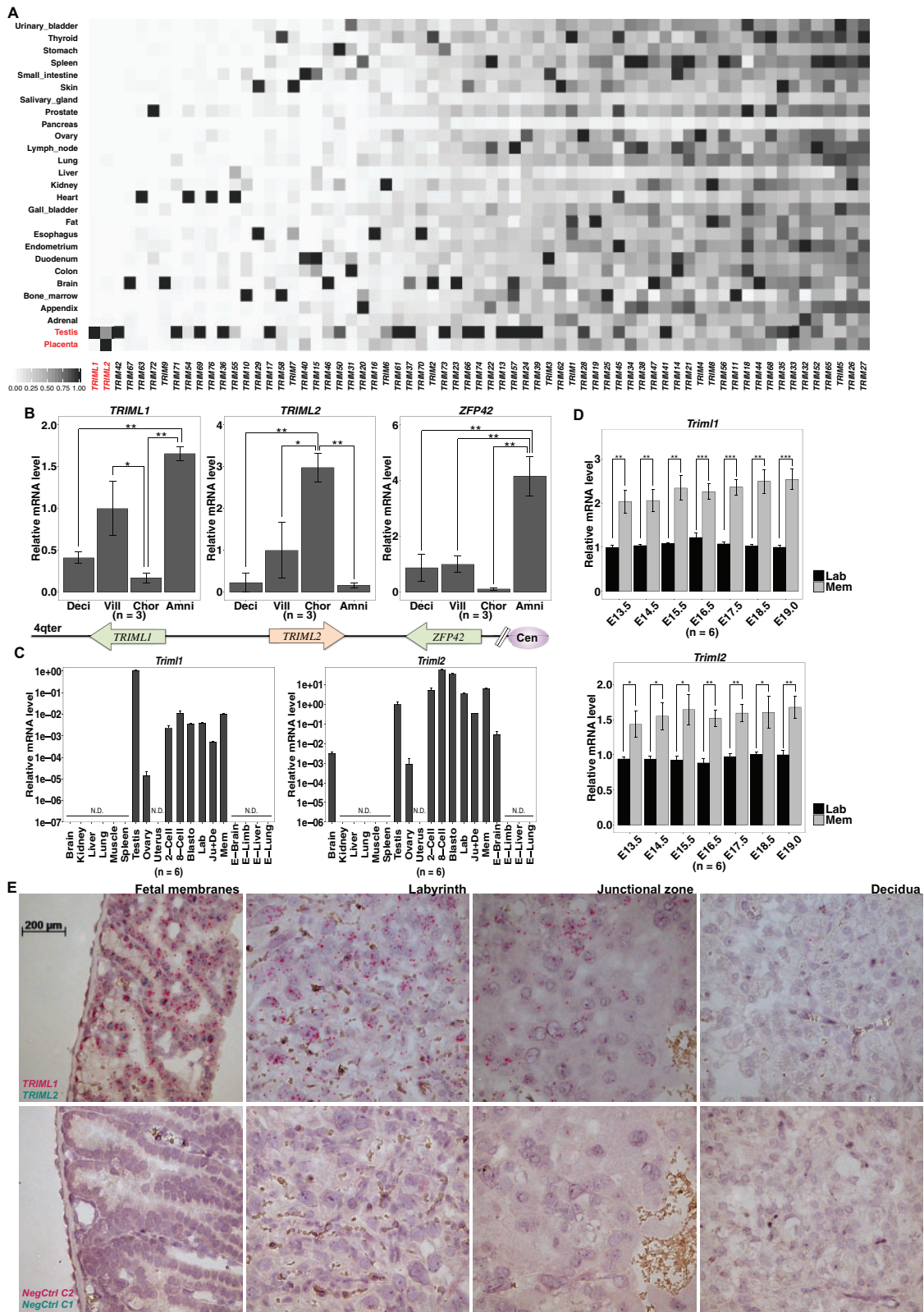


**Fig. 2.** *TRIML1* and *TRIML2* show different restricted expression patterns. (A) Heatmap of relative tissue expression levels of human *TRIM* genes, showing restricted expression of *TRIML1* and *TRIML2* (data from the Human Protein Atlas, expression level in each tissue normalized to the highest RPKM for each *TRIM* gene, [supplementary fig. S4, Supplementary Material](#) online). (B) Preferential expression compartment of *TRIML1*, *TRIML2*, and *ZFP42* in extraembryonic tissues correlates with their transcribing direction. Expression levels normalized to placenta villi. Values are mean  $\pm$  SEM. One-way ANOVA, Tukey's HSD,  $^{***}P < 0.01$ ,  $^{**}P < 0.05$ . Deci, placental decidua; Vill, placental villi; Chor, chorion; Amni, amnion; Cen, centromere; 4qter, terminal of chromosome 4 long arm; arrows indicate the transcription direction of each gene. (C) *Triml1* and *Triml2* expression in adult and embryo mouse tissue show restricted expression in preimplantation embryo, extraembryonic tissues, testis, and ovary. Expression

lower than in testis and the expression of either gene was not detected in the nonpregnant uterus, nor in regions of pregnant uterus away from the implantation sites (fig. 2C). Thus in both human and mouse, *TRIML1* and *TRIML2* show restricted expression—yet with significant differences, as *TRIML1* shows highest expression in adult testis, while *TRIML2* is preferentially expressed in preimplantation embryos and in trophoblast-derived structures.

### *TRIML1* and *TRIML2* Expression Are Differentially Regulated during Trophoblast Differentiation

The differences between tissue distribution of *TRIML1* and *TRIML2* suggest that they may have acquired different cis-regulatory elements that can facilitate the acquisition of novel functions (Zhang and Zhou 2019). Although *TRIML1* and *TRIML2* reside in the same gene cluster, their head-to-head arrangement allows direction-sensitive cis-regulatory elements to influence their expression differently (Ibrahim et al. 2018; Mikhaylichenko et al. 2018). Indeed, the preferred compartment of expression within human fetal membrane appears to correlate with the direction of gene transcription, as *TRIML2*, which locates on the negative strand, shows highest expression in chorion, while the genes on the positive strand, *TRIML1* and *ZFP42* (the third gene in this gene cluster), show highest expression in amnion (figs. 1A and 2B), supporting the existence of direction-sensitive cis-regulatory elements. Therefore, we tested the hypothesis that *TRIML1* and *TRIML2* expression are differentially regulated, by examining their expression dynamics during trophoblast differentiation. Forskolin can induce BeWo choriocarcinoma cells to undergo cell fusion in a process similar to placenta syncytiotrophoblast formation (Muroi et al. 2009). Both *TRIML1* and *TRIML2* are expressed in BeWo cells (supplementary fig. S5 and table S1, Supplementary Material online). The mRNA abundance of both *TRIML1* and *TRIML2* after 6 h of forskolin treatment show significant downregulation compared with the control groups treated only with the solvent DMSO (one-way ANOVA, Tukey's HSD, DMSO vs. 50  $\mu$ M forskolin  $P < 0.001$ , DMSO vs. 100  $\mu$ M forskolin  $P < 0.001$ ) (fig. 3A). After 36 h of forskolin treatment, *TRIML1* is still significantly downregulated in all treated groups. However, no statistically significant differences of *TRIML2* remain between forskolin-treated groups and DMSO control groups, suggesting the regulation of *TRIML2* expression is highly time-sensitive (one-way ANOVA, Tukey's HSD; *TRIML1*: DMSO vs. 50  $\mu$ M forskolin  $P < 0.001$ , DMSO vs. 100  $\mu$ M forskolin  $P < 0.001$ ; *TRIML2*:  $P = 0.51$ ) (fig. 3B).

One caveat of using BeWo cells is that the expression pattern changes observed in carcinoma cell lines may reflect the process specific to malignancy rather than normal

trophoblast differentiation. Therefore, we verified the results in mouse trophoblast stem cells (TSCs), which can be differentiated to syncytiotrophoblast layer II (SynT-II) in vitro by canonical Wnt pathway activation, using specific GSK3 $\beta$  inhibitor, GSK3ixv (Zhu et al. 2017). GSK3ixv treatment significantly downregulated both *Triml1* and *Triml2* at 24 h compared with TSCs cultured with proliferation media and DMSO solvent (one-way ANOVA, Tukey's HSD; *Triml1*: proliferation media vs. 0.2  $\mu$ M GSK3ixv  $P < 0.001$ , proliferation media vs. 0.4  $\mu$ M GSK3ixv  $P < 0.001$ ; *Triml2*: proliferation media vs. 0.2  $\mu$ M GSK3ixv,  $P < 0.05$ ) (fig. 3C). This downregulation persisted at 96 h for both *Triml1* and *Triml2* (one-way ANOVA, Tukey's HSD; *Triml1*: proliferation media vs. 0.2  $\mu$ M GSK3ixv  $P < 0.001$ , proliferation media vs. 0.4  $\mu$ M GSK3ixv  $P < 0.001$ ; *Triml2*: proliferation media vs. 0.2  $\mu$ M GSK3ixv  $P < 0.05$ , proliferation media vs. 0.4  $\mu$ M GSK3ixv  $P < 0.01$ ) (fig. 3D). Thus in both human choriocarcinoma BeWo cell line and in mouse TSCs, syncytialization reduces expression of *TRIML1*, which is consistent with the low *TRIML1* expression level observed in term human placenta. Although *TRIML2* did not show sustained downregulation in BeWo, its expression is significantly reduced as mouse TSCs differentiate to SynT-II cells. This difference may reflect the difference between the anatomy of mouse and human interhemal membranes. The mouse interhemal membrane consists of two layers of SynTs, while the human interhemal membrane consists of only one layer of SynTs (Coan et al. 2005). Syncytin b, the fusogenic protein in mouse SynT-II is closely related to syncytin-2 in human cytotrophoblasts, the less differentiated trophoblasts that continuously fuse to syncytiotrophoblasts (Imakawa and Nakagawa 2017). The downregulation of *Triml2* observed in mouse SynT-II may correspond to the transient *TRIML2* downregulation during BeWo cell fusion (fig. 3A). Thus, *TRIML1* and *TRIML2* may be regulated differently during trophoblast differentiation, especially toward the final stage of syncytialization.

### *TRIML2* Attenuates Trophoblast Proinflammatory Cytokine Production and Promotes Trophoblast Survival

As *TRIML1* and *TRIML2* may be differentially regulated during trophoblast differentiation, we tested whether their expression responds differently to activation of proinflammatory pathways in trophoblasts. Previous studies have shown that many TRIMs can be induced during antiviral immune responses (Carthagen et al. 2009). Viruses are a driving force involved in both TRIM gene family expansion, as well as the evolution of eutherian placentation (Si et al. 2006; Imakawa and Nakagawa 2017). We used poly(I:C), a synthetic analog of

Fig. 2. Continued

levels normalized to placental villi. N.D., not detected; 2-Cell, 2-cell stage embryo; 8-Cell, 8-cell stage embryo; Blasto, blastocyst; Lab, E15.5 labyrinth; Ju+De, E15.5 junctional zone, and decidua; Mem, E15.5 fetal membranes; E-Brain, E15.5 embryo brain; E-Limb, E15.5 embryo limb; E-Liver, E15.5 embryo liver; E-Lung, E15.5 embryo lung. (D) *Triml1* and *Triml2* show higher expression in fetal membrane than in placental labyrinth. Expression levels normalized to E19.0 labyrinth. Values are mean  $\pm$  SEM. *t*-Test, \*\*\* $P < 0.001$ , \*\* $P < 0.01$ , \* $P < 0.05$ . (E) RNAScope assay showing *Triml1* and *Triml2* expression in extraembryonic structures, upper row: signal from *Triml1* and *Triml2*-specific probes, lower row: nonspecific signals from negative control probes.

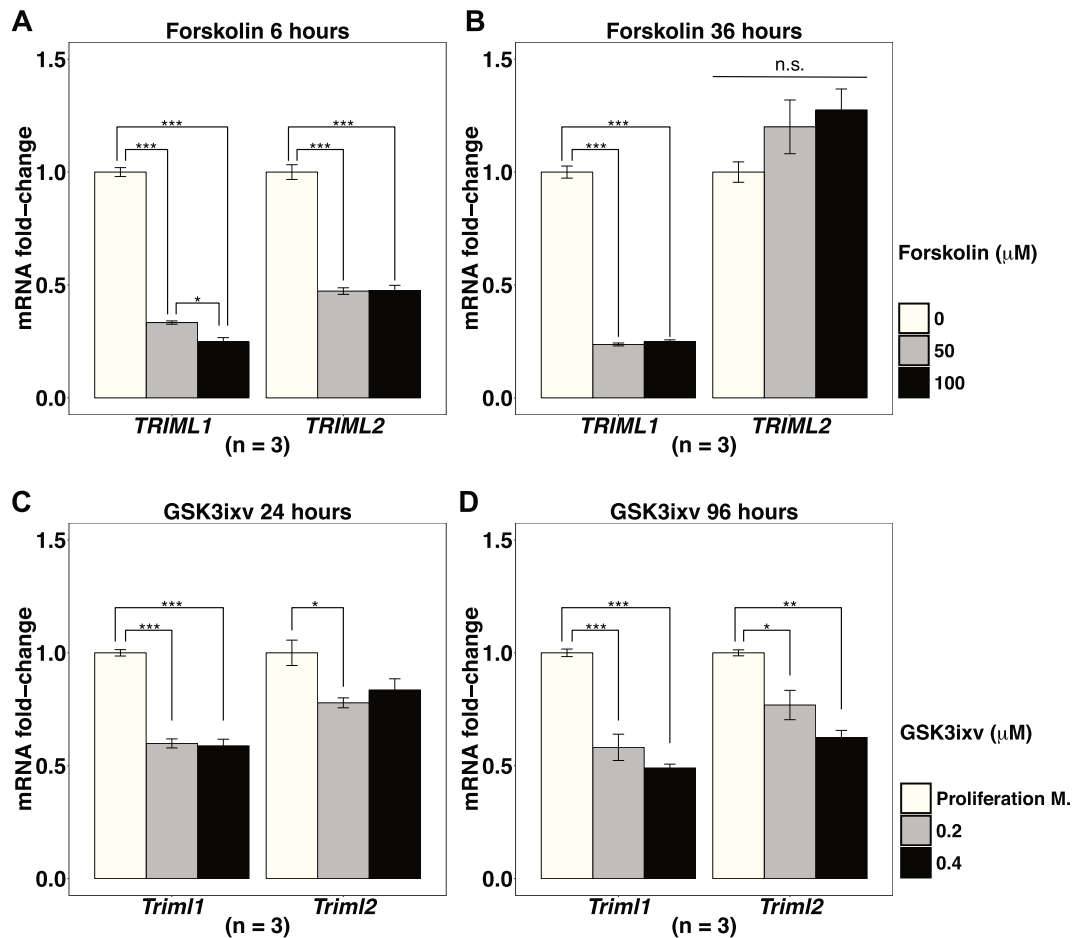


**Fig. 3.** *TRIML1* and *TRIML2* expression during trophoblast differentiation. (A and B) *TRIML1* and *TRIML2* expression differ during forskolin-induced BeWo cell syncytialization. (C and D) GSK3ixv-induced mouse TSCs differentiation into syncytiotrophoblast layer II causes downregulation of both *Triml1* and *Triml2*. Expression levels normalized to control groups. Values are mean  $\pm$  SEM. One-way ANOVA, Tukey's HSD, \*\*\* $P < 0.001$ , \*\* $P < 0.01$ , \* $P < 0.05$ . n.s., not statistically significant.

dsRNA, to simulate viral infection associated proinflammatory pathway activation. Since transfection reagent alone causes downregulation of both *TRIML1* and *TRIML2* in BeWo cells (data not shown), we used JEG3 choriocarcinoma cells, which also express both *TRIML1* and *TRIML2* (supplementary fig. S5 and table S1, Supplementary Material online), to test this hypothesis. Poly(I:C) transfection in JEG3 induced 2-fold upregulation of *TRIML2* at 6 h ( $t$ -test,  $P < 0.001$ ) and 12-fold upregulation at 24 h ( $t$ -test,  $P < 0.05$ ), compared with control groups treated only with transfection reagent. *TRIML1* did not show significant response to poly(I:C) treatment (fig. 4A and B).

We then tested *TRIML1* and *TRIML2*'s influence on the expression of cytokines. Using gene targeting siRNAs, we achieved  $78.4\% \pm 3.3\%$  (in control groups treated with transfection reagent alone) and  $79.4\% \pm 4.0\%$  (in groups transfected with poly(I:C)) reduction of *TRIML1* mRNA and  $82.4\% \pm 0.4\%$  (in control groups treated with transfection reagent alone) and  $69.3\% \pm 4.0\%$  (in groups transfected with poly(I:C)) reduction of *TRIML2* mRNA, compared with control siRNA-treated groups ( $n = 3$ , mean  $\pm$  SD). At baseline, neither *TRIML1* nor *TRIML2* siRNA treatment caused any

significant differences in *interferon beta 1* (*IFNB1*) expression compared with control siRNA-treated groups (one-way ANOVA,  $P = 0.373$ ). Upon poly(I:C) treatment however, siRNA knockdown of *TRIML2* caused 2-fold upregulation in *IFNB1* (one-way ANOVA, Tukey's HSD, *TRIML2* siRNA vs. control siRNA,  $P < 0.001$ ) (fig. 4C).

*IL6* is upregulated in preimplantation embryo during the implantation window (Basak et al. 2002). However, elevated serum *IL6* is associated with spontaneous abortion in both human and mouse (Zenclussen et al. 2000, 2003). *TRIML2* knockdown significantly decreased baseline *IL6* expression in JEG3 (one-way ANOVA, Tukey's HSD, *TRIML2* siRNA vs. control siRNA,  $P < 0.01$ ). But upon poly(I:C) treatment, *TRIML2* knockdown resulted in 1.7-fold upregulation of *IL6* (one-way ANOVA, Tukey's HSD, *TRIML2* siRNA vs. control siRNA,  $P < 0.01$ ) (fig. 4D).

Although proinflammatory cytokines produced by trophoblasts may contribute to implantation, excessive inflammation in trophoblasts causes cell death, and is associated with pregnancy loss (Johnson et al. 1993; Aldo et al. 2010). At baseline, no difference in cell survival was observed among *TRIML1*, *TRIML2*, and control siRNA-treated groups (one-way

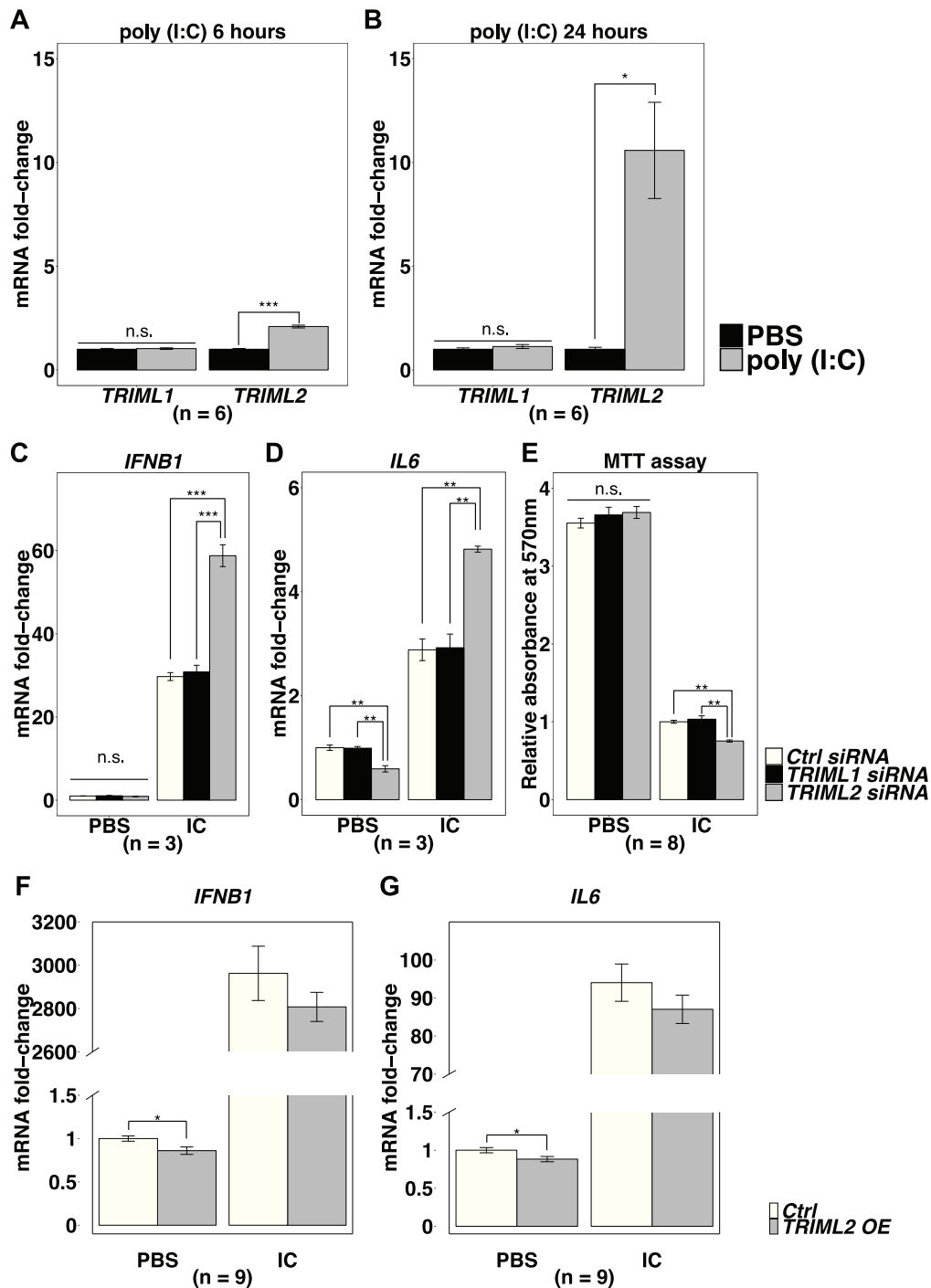


**Fig. 4.** *TRIML2* during trophoblast inflammation. (A and B) *TRIML2* expression in JEG3 is induced by poly(I:C). (C–E) *TRIML2* knockdown during inflammation causes increased expression of proinflammatory cytokines *IFNB1* (C) and *IL6* (D), and decreased survival of JEG3 cells (E). *TRIML2* overexpression reduces *IFNB1* (F) and *IL6* (G) expression at baseline. Normalized to PBS-treated control groups; IC, poly(I:C), OE, overexpression. Values are mean  $\pm$  SEM. (A, B, F, and G), *t*-test. (C and D) One-way ANOVA, Tukey's HSD. Poly(I:C) treatment in (E), Kruskal–Wallis test, Bonferroni post hoc correction. \*\*\* $P < 0.001$ , \*\* $P < 0.01$ , \* $P < 0.05$ . n.s., not statistically significant.

ANOVA,  $P = 0.46$ ). However, upon poly(I:C) transfection, *TRIML2* knockdown significantly reduced JEG3 survival (Kruskal–Wallis test, Bonferroni post hoc correction, *TRIML2* siRNA vs. control siRNA,  $P < 0.01$ ) (fig. 4E).

As reduced cell survival with *TRIML2* knockdown is observed, especially during poly(I:C) transfection, it is possible that the increased proinflammatory cytokine level reflected

the generally compromised cell function and the breakdown of homeostasis. To test whether *TRIML2* is directly involved in proinflammatory pathway regulation, we transfected JEG3 with a human *TRIML2* expression plasmid and achieved a  $3.7 \pm 0.2$ -fold increase of *TRIML2* mRNA at baseline, and  $11.3 \pm 0.6$ -fold increase during poly(I:C) transfection compared with control groups transfected with the

corresponding vector plasmid ( $n = 9$ , mean  $\pm$  SD). Due to the highly efficient vector transfection, *TRIML2* overexpression was achieved with reduced dosage of the transfection reagent, which significantly decreased cell death and improved cell function as reflected by the higher fold increment in the proinflammatory cytokine production upon poly(I:C) stimulation compared with siRNA-treated groups. At baseline, both *IFNB1* and *IL6* were significantly decreased by *TRIML2* overexpression ( $t$ -test,  $P < 0.05$ ). During poly(I:C) transfection, both *IFNB1* and *IL6* show trends of downregulation in *TRIML2* overexpressed groups, however, the differences are not statistically significant ( $t$ -test; *IFNB1*:  $P = 0.097$ ; *IL6*:  $P = 0.457$ ) (fig. 4F and G). *TRIML2* overexpression during poly(I:C) transfection also increased the survival of JEG3 cells by 2.3% ( $n = 9$ ,  $t$ -test,  $P = 0.039$ ). These results lend further support to the hypothesis that *TRIML2* is specifically regulated, participates in the attenuation of proinflammatory pathway in trophoblast, and promotes trophoblast survival, especially during viral infection.

### PRY/SPRY Domain of TRIML2 Shows Signature of Significant Positive Selection

The function of TRIMs closely correlates to their structure. We searched the conserved domains of *TRIML1* and *TRIML2* by RPS-BLAST (Marchler-Bauer et al. 2015) and COILS (Lupas et al. 1991), and found that, compared with their monotreme and marsupial homologs, eutherian *TRIML1* lack the B-box domain, while *TRIML2* lack both the B-box and the RING domains (fig. 5A). As *TRIML2* lack both the RING and B-box domains that may adopt RING-like folds (as in the case of the RING-less *TRIM16*; Bell et al. 2012), it is unlikely that *TRIML2* participates in the downregulation of proinflammatory pathway by acting as an E3 ubiquitin ligase. Previous studies show that TRIMs can form homo/hetero oligomers through the coiled-coil domain, and this process can dramatically influence their catalytic function (Sanchez et al. 2014). It is possible that *TRIML2* interacts with other TRIMs via its coiled-coil domain, and, by influencing the E3 function of other classical TRIMs, indirectly regulates the activity of proinflammatory pathways, such as the interferon pathway. Thus *TRIML2* may fine-tune the activity of ubiquitination signaling pathway without preserving its own enzymatic function. We suggest this may relax the selective constraint on *TRIML2*. To test the hypothesis of relaxed constraint, we modeled the dN/dS ratio ( $\omega$ ) of the homologous regions of eutherian *TRIML1* and *TRIML2* based on the phylogenetic tree generated through TimeTree website (Kumar et al. 2017; supplementary fig. S1, Supplementary Material online). Comparing the fit of one-ratio model ( $M_0$ ), which assigns the same  $\omega$  to both *TRIML1* and *TRIML2*, with the fit of a two-ratio model ( $M_2$ ), which allows  $\omega$  parameters to differ between *TRIML1* and *TRIML2*,  $M_2$  gives a significantly better fit than  $M_0$ , with *TRIML2*  $\omega$  (0.437) significantly higher than that of *TRIML1* (0.168), supporting a relaxed selection constraint on *TRIML2* (table 1).

As genes under relaxed selection constraint have been shown to contribute to evolutionary diversification (Hunt et al. 2011), we hypothesized that some sites of *TRIML2* may show evidence of adaptive evolution. We used two

sets of site models (comparison between  $M_{1a}$  nearly neutral and  $M_{2a}$  positive selection, and comparison between  $M_{7\beta}$  and  $M_{8\beta\&\omega}$ ) to test the hypothesis, and then used Bayes empirical Bayes (BEB) approach implemented in models  $M_{2a}$  and  $M_{8\beta\&\omega}$  to identify sites evolving under positive selection. Both  $M_{2a}$  and  $M_{8\beta\&\omega}$  fit the data for *TRIML2* significantly better than their corresponding neutral selection models (table 1). BEB detected twelve sites with posterior probabilities for  $\omega > 1$  greater than 95%. Ten of the twelve sites are located within the region homologous to the monotreme and marsupial TRIMs' B-box domain, the hinge region of the coiled-coil domain and the PRY/SPRY domain (fig. 5A and supplementary table S2, Supplementary Material online). Interestingly, the only site under significant positive selection in *TRIML1* (122 A in human ortholog) resides within the region that is homologous to the B-box domain of monotreme and marsupial TRIMs. Two additional sites within the region (114 A and 126 H) also suggest positive selection, although the posterior probabilities of these two sites having  $\omega > 1$  do not reach statistical significance (supplementary table S2, Supplementary Material online). The substitution by alanine at residue 114 altered the last cysteine in the CHC3H2 Zinc finger in the B-box domain, suggesting that the loss of B-box in eutherian TRIMs is under positive selection.

Another domain in *TRIML2* with multiple positively selected sites is the PRY/SPRY domain. Previous studies have resolved the protein structure of the PRY/SPRY domains of several TRIMs including the retrovirus-restricting *TRIM5*, and identified a canonical binding interface.  $\beta$ -sheets form the conserved hydrophobic core of this canonical binding interface. Variable loops (VLs), which show great variation among TRIMs, connect these conserved  $\beta$ -sheets. Among these VLs, the N-terminal of VL3 forms the variable region 2 (v2) with the last C-terminal residue of  $\beta_5$  immediately in front. V2 is known to contribute to the determination of retrovirus restriction specificity of *TRIM5* (James et al. 2007). Alignment of human *TRIML2* and *TRIM5* revealed that two of the three PRY/SPRY sites under significant positive selection and four additional residues that also show evidence of positive selection all reside within v2, with  $\beta_4$ , one of the most conserved regions in eutherian *TRIML2*, in vicinity (fig. 5B). By analogy, these results suggest that the selection in *TRIML2* may act on its ability to interact with viruses. As integration of genes and/or regulatory elements originating from retroviruses has made significant contributions to the evolution and diversification of eutherian placentation (Chuong et al. 2013; Imakawa and Nakagawa 2017), by influencing defense against retroviruses, *TRIML2* may participate in the selection of retroviruses that become incorporated into the host genome, and through coevolution with retroviruses, indirectly influence the evolution and diversification of eutherian placentation. We tested the hypothesis that the PRY/SPRY domain is under different selection among species with different placentation traits by comparing the one-ratio model ( $M_0$ ) to the two-ratio/three-ratio models ( $M_2$ ), which allow branches with different placental interdigitation/invasiveness to have different  $\omega$  parameters (see supplementary fig. S1, Supplementary Material online, for phylogenetic tree generated through TimeTree



**Table 1.**  $\omega$  and Likelihood Ratio Test (LRT) of Eutherian *TRIML1* and *TRIML2*.

| Gene Region  | Model                 | Parameters   | lnL <sup>a</sup> | P Value  |
|--|-----------------------|--|------------------|----------|
| Homologous region of <i>TRIML1</i> and <i>TRIML2</i> | M0                    | $\omega = 0.2983$  | -29,277.6        | 4.58e-65 |
|  | M2                    | $\omega T1 = 0.168$<br>$\omega T2 = 0.437$   | -29,132.5        |          |
| Homologous region of <i>TRIML1</i>                   | M1a                   | $p1 = 0.8288, \omega1 = 0.095$<br>$p2 = 0.1712, \omega2 = 1.000$                                   | -17,649.8        | 1.00     |
|  | M2a                   | $p1 = 0.8288, \omega1 = 0.095$<br>$p2 = 0.1712, \omega2 = 1.000$<br>$p3 = 0.0000, \omega3 = 1.933$ | -17,649.8        |          |
|  | M7 $\beta$            | $p = 0.3580, q = 1.6188$   | -17,483.4        | 0.008    |
|  | M8 $\beta$ & $\omega$ | $p0 = 0.9785, p = 0.4073$<br>$q = 2.2013, (p1 = 0.0215)$<br>$\omega = 1.094$                       | -17,478.6        |          |
| Homologous region of <i>TRIML2</i>                   | M1a                   | $p1 = 0.5441, \omega1 = 0.234$<br>$p2 = 0.4559, \omega2 = 1.000$                                   | -24,785.1        | 1.14e-8  |
|  | M2a                   | $p1 = 0.5254, \omega1 = 0.237$<br>$p2 = 0.4285, \omega2 = 1.000$<br>$p3 = 0.0460, \omega3 = 1.956$ | -24,766.8        |          |
|  | M7 $\beta$            | $p = 0.7472, q = 0.7273$   | -24,821.7        | 9.63e-16 |
|  | M8 $\beta$ & $\omega$ | $p0 = 0.8591, p = 1.0102$<br>$q = 1.3469, (p1 = 0.1409)$<br>$\omega = 1.438$                       | -24,787.1        |          |
| <i>TRIML1</i> PRY/SPRY                               | M0                    | $\omega = 0.083$   | -5,936.0         | 0.236    |
|  | M2                    | $\omega Lab = 0.089,$<br>$\omega Vil = 0.074$  | -5,935.3         |          |
|  | M2                    | $\omega Hemo = 0.077$<br>$\omega Endo = 0.080$<br>$\omega Epi = 0.111$                             | -5,934.2         | 0.161    |
| <i>TRIML2</i> PRY/SPRY                               | M0                    | $\omega = 0.421$   | -9,476.6         | 0.039    |
|  | M2                    | $\omega Lab = 0.451$<br>$\omega Vil = 0.365$   | -9,474.5         |          |
|  | M2                    | $\omega Hemo = 0.439$<br>$\omega Endo = 0.370$<br>$\omega Epi = 0.407$                             | -9,475.8         | 0.419    |

lnL, log likelihood values;  $\omega T1$ ,  $\omega$  of *TRIML1* branches;  $\omega T2$ ,  $\omega$  of *TRIML2* branches;  $\omega Lab$ ,  $\omega$  of labyrinthine and lamellar branches;  $\omega Vil$ ,  $\omega$  of villous and trabecular branches;  $\omega Hemo$ ,  $\omega$  of hemochorial branches;  $\omega Endo$ ,  $\omega$  of endotheliochorial branches;  $\omega Epi$ ,  $\omega$  of epitheliochorial branches.

explanation, that *TRIML2* arose from a gene duplication event in the eutherian and marsupial common ancestor, followed by eutherian-specific gene fixation and marsupial-specific gene loss, cannot be entirely ruled out (fig. 1E). Some degree of caution should be taken with the phylogenetic reconstruction due to the scarcity of marsupial and monotreme genomes and potential genome assembly and/or gene annotation errors associated with draft genomes. However, despite the uncertainty regarding the evolutionary origin of the RING-less *TRIML2*, its absence in marsupial genomes and ubiquitous preservation in eutherian genomes still indicates that it contributes to the evolutionary divergence of eutherian and marsupial.

Duplicated genes that are preserved in the genome may go through either neofunctionalization or subfunctionalization. A common signature of gaining new functions is the establishment of new expression pattern via recruitment of new cis-regulatory elements (Zhang and Zhou 2019). Although both *TRIML1* and *TRIML2* show highly restricted tissue distribution, they differ in their specific expression compartments. The highest expression of *TRIML1* is in adult testis, followed by preimplantation embryos and extraembryonic tissues derived from inner cell mass, such as amnion.

*TRIML2* shows higher expression in fetal than adult tissues, and in extraembryonic tissues it shows higher expression in trophoblast-derived tissues, such as chorion (fig. 2). The divergence in expression compartments of the *TRIMLs* parallels the divergence in direction of transcription, as *TRIML1* shows greater similarity to the expression pattern of *ZFP42*, the third member in the gene cluster which transcribes in the same direction as *TRIML1* but opposite to *TRIML2* (fig. 2B). Previous studies have shown that neighboring genes can share cis-regulatory elements such as enhancers (Quintero-Cadena and Sternberg 2016). As *ZFP42* encodes REX-1, an embryonic stem cell (ESC) pluripotency marker (Scotland et al. 2009), it is possible that by sharing direction-sensitive cis-regulatory elements, such as unidirectional/skewed enhancers (Ibrahim et al. 2018; Mikhaylichenko et al. 2018), *TRIML1* establishes preferred expression in structures derived from ESCs, while the acquisition of direction-sensitive trophoblast-specific cis-regulatory elements by *TRIML2* further separated the expression patterns. Indeed, BMP4-induced differentiation of human ESCs to trophoblast significantly upregulates *TRIML2*, while *TRIML1* shows a trend toward downregulation (GSE30915, Marchand et al. 2011). Downregulation of *TRIML1* also accompanies the differentiation of BeWo cells

(fig. 3A and B), supporting the divergence of *TRIML1* and *TRIML2* expression patterns, which may facilitate the divergence of their functions.

Although *TRIML2* is preferentially expressed by trophoblasts, its expression is constitutively higher in fetal membranes (fig. 2D), where excessive inflammation is especially detrimental to the maintenance of pregnancy (Chavan et al. 2017). *TRIML2* may be transiently downregulated at the early stage of trophoblast differentiation (fig. 3), which may reduce the interference with the generation of proinflammatory cytokines necessary for initial placental development. *TRIML2* expression is induced by activation of proinflammatory pathways in trophoblast (fig. 4A and B). These expression patterns fit what would be expected for genes fine-tuned for the regulation of inflammation in trophoblast.

Functionally, losing the catalytic RING domain may facilitate the preservation of *TRIML2* in the genome through sub-functionalization. Losing most of the catalytic function may also enable *TRIML2* to function as a dominant inhibitor of the inflammatory pathway, as illustrated by the increased proinflammatory cytokine production and reduced trophoblast survival during its knockdown, and reduced proinflammatory cytokine production and increased cell survival during its overexpression (fig. 4). A recent study has shed light on the potential mechanisms through which *TRIML2* promotes cell survival. *TRIML2* knockdown in human oral squamous carcinoma cells upregulates p27<sup>Kip1</sup>, a cyclin-dependent kinase inhibitor and apoptosis inducer that can be induced by TP53 (Wang et al. 1997; Hayashi et al. 2019). Interestingly, *TRIML2* can be induced by TP53 Arg72 variants, but not by Pro72 variants (Kung et al. 2015). Higher risks of recurrent implantation failure and recurrent pregnancy loss are associated with TP53 Pro72 variants when compared with Arg72 variants (Kang and Rosenwaks 2018). It is intriguing to consider whether the lack of efficient induction of *TRIML2* by TP53 Pro72 variants may result in abnormally high level of p27<sup>Kip1</sup>, which in turn may cause excessive apoptosis of trophoblasts, thus contributing to the increased risk of adverse pregnancy events. As the establishment and maintenance of pregnancy involve complex interplay between multiple cell types of mother and fetus, animal models with modified TP53 and/or *TRIML2* genes may provide more information for understanding the mechanisms and differentiating the maternal/fetal contributions to the increased risk.

As similar inflammatory pathways underlie both eutherian implantation and host immunity against infectious pathogens such as viruses (Mor and Cardenas 2010; Griffith et al. 2017), the anti-inflammatory function of *TRIML2* that facilitates the accommodation of the embryo at the maternal-fetal interface may also relax the stringency on viral activities at such locations. A recent study shows that *TRIML2* upregulation during Kaposi's sarcoma-associated herpes virus activation in lymphoma cell line BCBL-1 is associated with both increased virion production and prolonged host cell survival (Gu et al. 2018). Considering the striking similarities between proliferation and invasion behaviors of trophoblast and cancer cells (Ferretti et al. 2006), a certain level of tolerance to viral activities within the placenta, a transient organ, could be

beneficial compared with a full-blown immune response that may interrupt the quiescence at the maternal-fetal interface. Indeed, eutherian placenta shows substantial tolerance to retroviruses/endogenous retroviruses (ERVs) (Haig 2012; Chuong 2013). Furthermore, repeated co-option of both protein-coding genes and regulatory elements originating from ERVs play a crucial role in the rapid evolution of eutherian placentation (Haig 2012; Chuong et al. 2013; Imakawa and Nakagawa 2017). Functioning as a negative regulator, the RING-less *TRIML2* may contribute to establishing an accommodating environment for retroviruses/ERVs. However, as "selfish parasites," retroviruses/ERVs can be costly to the host, therefore, host defense mechanisms that participate in the selection of retroviruses/ERVs likely experience adaptive evolution (Haig 2012). Several amino acid residues of *TRIML2* show a signature of positive selection, especially in the TRIM-interacting coiled-coil domain and the substrate-binding PRY/SPRY domain (fig. 5A and supplementary table S2, Supplementary Material online). Coiled-coil domain-mediated dimerization can dramatically influence TRIMs' catalytic function (Sanchez et al. 2014). In some retroviral-restricting TRIMs, such as TRIM5 $\alpha$ , subsequent higher-order association can result in the formation of a hexagonal lattice that matches the lattice formed by viral capsid and significantly restrict the activities of the retroviruses (Ganser-Pornillos et al. 2011). Substituting TRIM monomers in such lattices through its coiled-coil domain, *TRIML2* could interrupt the orderly structure necessary for the retroviral-restricting function. Changes in *TRIML2*'s PRY/SPRY domain may change its affinity to the viral capsid thus influencing the selection of retroviruses that can escape the restrictions imposed by other TRIMs.

Previous studies suggest lineage-specific ERV enhancer co-option may be the mechanism underlying the evolution of eutherian placentation diversification (Chuong et al. 2013). Corresponding to different placentation features, we observed different selection pressure of the potential virus-interacting PRY/SPRY domain of *TRIML2*. Significantly higher  $\omega$  is associated with placentas with higher levels of interdigitation and vice versa (table 1). Higher-level interdigitation such as in labyrinthine placentation provides larger surface area for exchange between mother and fetus, and therefore can support faster fetal growth. On the other hand, rapid draining of maternal resources can exacerbate the parental-offspring-conflict (Capellini 2012; Garratt et al. 2013). Therefore, we suggest that the higher  $\omega$ , associated with higher-level placental interdigitation, may reflect the intensified parental-offspring conflict, as the plasticity of *TRIML2*, resulting from relaxed selection, may facilitate the rapid modification of antiviral immune response by adjusting the expression of proinflammatory cytokines at the maternal-fetal interface. Some of these proinflammatory cytokines, such as IFN $\beta$ 1 (Jablonska et al. 2010) and IL6 (Gopinathan et al. 2015), likely participate in the regulation of angiogenesis, arguably resulting in rapid modification of the degree of placental interdigitation. In another prominent placentation trait, placental invasiveness, the highest  $\omega$  is associated with hemochorial placentation, although the difference does not reach

statistical significance (table 1). The high  $\omega$  in hemochorial placentation may reflect the challenge in maintaining maternal immune tolerance in highly invasive placentas in which fetal tissue are directly exposed to maternal blood stream (Elliot and Crespi 2006).

The plasticity of TRIML2 renders high tolerance to non-synonymous substitutions. Indeed, the Exome Aggregation Consortium (ExAC) database predicts the index of intolerance to loss of function (LoF) of TRIML2 to be 0.00 (range 0–1, with 0 most tolerant) (Lek et al. 2016). We suggest that the modifiable nature of TRIML2, with tolerance even to loss of function (at least under some conditions), may increase its variation and provide a reservoir for potential coevolution with retroviruses/ERVs that may contribute to the diversification of eutherian placentation. Eutherian placenta is one of the most diverse organs despite its similar and essential core functions across species (Garratt et al. 2013). “Nonessential” immune genes, that is, genes that are only necessary when host is challenged by corresponding pathogens, are amongst the fastest evolving genes, a phenomenon likely driven by the host-parasite coevolution that favors the diversification of these immune genes (Hurst and Smith 1999). We suggest that many nonessential immune genes may participate in the coevolution with retroviruses/ERVs that results in the diversification of eutherian placentation. Through gene duplication, the TRIM family may provide many such modifiable genes, as the TRIM family shows fast expansion in the eutherian lineage and sublineages (Versteeg et al. 2014). We examined the LoF index of human TRIMs that were predicted to originate in Eutherian or sublineages (Capra et al. 2013). Out of 23 TRIMs that have records in ExAC database, the LoF index of 14 is predicted to be 0.00 (Lek et al. 2016; supplementary table S3, Supplementary Material online), including TRIMs such as TRIM5 (Ganser-Pornillos et al. 2011) and TRIM6 (Bharaj et al. 2017), that have been shown to play important roles in antiviral immunity. Through interaction with TRIMs with placentally biased expression, and/or alternative splicing that can result in the RING-less negative regulatory forms (Versteeg et al. 2013), these TRIMs may selectively permit the activity of some retroviruses/ERVs at the maternal-fetal interface, without interfering with the host’s overall antiviral immunity. Thus, the fast-evolving and versatile TRIM family may provide a wealth of evolvability in the regulation of the selective permissive placental environment to retroviruses/ERVs (Chuong 2013) and contribute to the fascinating diversification of eutherian placentation.

## Conclusion

The eutherian-specific gene TRIML2 functions as a regulatory inhibitor of the proinflammatory cytokine production pathways in trophoblasts. We suggest that this function contributes to the establishment of the anti-inflammatory phase critical for eutherian implantation and prolonged pregnancy, and by influencing antiviral immunity against coevolving retroviruses/ERVs, also contributed to the diversification of placentation.

## Materials and Methods

### Phylogenetic Gene Tree Reconstruction and Inference of Selection

Information on placental interdigitation and invasiveness were obtained from Wildman et al. (2006), Elliot and Crespi (2009), and Garratt et al. (2013). The protein coding DNA sequences for TRIML1 and TRIML2 of species with known placental interdigitation and invasiveness were downloaded from NCBI Entrez Nucleotide sequences through Alignment Explorer implemented in MEGA X (Kumar et al. 2018), the integrity of the coding regions were reviewed and partial sequences were removed from analysis. SPRY domain was inferred by RPS-BLAST (Marchler-Bauer et al. 2015). Sequences were aligned using MUSCLE implemented in MEGA X. Conserved blocks from multiple alignments suitable for phylogenetic analysis were selected using Gblocks v0.91b (Castresana 2000). Phylogenetic tree was inferred by maximum likelihood with 1,000 bootstraps implemented in MEGA X and by Bayesian analyses using MrBayes v3.1.2 (Ronquist and Huelsenbeck 2003). The CodeML package implemented in PAML 4.4 was used to estimate  $\omega$  (Yang 2007). All phylogenetic trees used for PAML analyses were generated through TimeTree website (Kumar et al. 2017). All selection models were compared with the neutral models using a likelihood ratio test (LRT) and null hypothesis was rejected when  $P < 0.05$ .

### Relative Tissue Expression Level of Human TRIM Genes

Tissue-specific RNA-Seq data for human TRIM genes was downloaded from the Human Protein Atlas, accessed through the gene portal of NCBI (last accessed October 19, 2017). For each TRIM gene, the expression level in each tissue was expressed as fraction of the amount in the tissue with highest expression level.

### Human Placenta and Fetal Membrane Samples

Three human placentas at term with attached fetal membranes were collected with IRB approval (IRB protocol: CCHMC IRB 2013–2243). Samples were washed with PBS prior to collecting three tissue samples from the villous side and three tissue samples from the decidual side of each placenta. Fetal membranes were manually separated into chorion and amnion, and six samples were collected from each part.

### Cell Lines

The mouse trophoblast stem cell line was provided by Dr S.K. Dey (Xie et al. 2012) and was cultured in DMEM/F12 medium supplemented with Activin A (R&D Systems 338-AC) (100  $\mu$ g/ml), heparin (1  $\mu$ g/ml), FGF4 (R&D Systems 235-F4) (25 ng/ml), 20% FBS, 2-Mercaptoethanol (100  $\mu$ M), sodium pyruvate (1 mM), glutaMAX (2 mM), penicillin (100 U/ml), and streptomycin (100  $\mu$ g/ml). BeWo choriocarcinoma cell line was obtained from ATCC (ATCC CCL-98) and cultured in DMEM/F12 medium supplemented with 10% FBS, glutaMAX (2 mM), penicillin (100 U/ml), and streptomycin

(100 µg/ml). JEG3 choriocarcinoma cell line was obtained from ATCC (ATCC HTB-36) and cultured in DMEM medium supplemented with 10% FBS, glutaMAX (2 mM), penicillin (100 U/ml), and streptomycin (100 µg/ml). All cell lines were cultured at 37 °C and 5% CO<sub>2</sub>.

### Mouse TSCs Differentiation

About 1 × 10<sup>4</sup> mouse TSCs were seeded per well of 6-well plate. About 24 h after seeding, medium without Activin A, heparin, and FGF4, and with 0.2 µM or 0.4 µM GSK3ixv (Millipore 361558) was added. Proliferation medium described above with the same volume of solvent DMSO was used as control. Medium was exchanged every 24 h. Total RNA was collected after 24 or 96 h.

### BeWo Cell Differentiation

About 2 × 10<sup>5</sup> BeWo cells were seeded per well of 6-well plate. About 48 h after seeding, culture medium was changed, and 50 µM, or 100 µM forskolin (Sigma F3917), or the same volume of solvent DMSO were added. Medium was exchanged every 24 h. Total RNA was collected after 6 or 36 h.

### Poly(I:C) Transfection

About 1 × 10<sup>5</sup> JEG3 cells were seeded per well of 6-well plate. About 48 h after seeding, culture medium was changed, and high molecular weight poly(I:C) (InvivoGen tlr1-pic) was transfected at a concentration of 2 µg/ml with 4 µl/ml Lipofectamine 3000 (Invitrogen) (Palchetti et al. 2015). PBS with 4 µl/ml Lipofectamine 3000 was added to control wells. Total RNA was collected after 6 or 24 h.

### RNA Interference with Poly(I:C) Transfection

About 2 × 10<sup>5</sup> JEG3 cells were seeded per well of 6-well plate. About 48 h after seeding, culture medium was changed, and siRNA for *TRIML1* (Invitrogen Silencer Select s50635), *TRIML2* (Invitrogen Silencer Select s47568), or control siRNA (Invitrogen Silencer Select Negative Control No. 2) were transfected at 100 pmol/well with 4 µl/ml Lipofectamine 3000. About 18 h after siRNA transfection, high molecular weight poly(I:C) was transfected at a concentration of 2 µg/ml with 4 µl/ml Lipofectamine 3000. PBS with 4 µl/ml Lipofectamine 3000 was added to control wells. Total RNA was collected 6 h after poly(I:C) treatment. [3-(4,5-dimethylthiazol-2-yl)-2,5-diphenyltetrazolium bromide] (MTT) assay was carried out 12 h after poly(I:C) treatment.

### *TRIML2* Overexpression with Poly(I:C) Transfection

About 1 × 10<sup>5</sup> JEG3 cells were seeded per well of 6-well plate. About 24 h after seeding, culture medium was changed, and human *TRIML2* expression plasmid (OriGene RC211281L1) or vector plasmid (OriGene PS100064) were transfected at 15 ng/well with 1.5 µl/ml Lipofectamine 3000. About 24 h after expression plasmid transfection, high molecular weight poly(I:C) was transfected at a concentration of 2 µg/ml with 4 µl/ml Lipofectamine 3000. PBS with 4 µl/ml Lipofectamine 3000 was added to control wells. Total RNA was collected 6 h after poly(I:C) treatment. MTT assay was carried out 12 h after poly(I:C) treatment.

### MTT Assay

JEG3 cells were treated as described earlier. Subsequently, cells were washed three times with 500 µl PBS/well. About 800 µl/well MTT solution at 0.5 mg/ml was added to each well, and incubated at 37 °C for 3 h. About 500 µl/well of DMSO was added and plate was wrapped in foil and shaken on an orbital shaker for 15 min. About 200 µl of the resulting solution from each well was transferred from 6-well plates to a well in 96-well plates and the absorbance was measured at 570 nm wavelength.

### BeWo and JEG3 Transcriptomes

BeWo and JEG3 cells were grown under above specified conditions until 90% confluent. Cells were harvested by scraping and the total RNA was extracted from cells using the RNeasy Mini kit (Qiagen) followed by on-column DNase I treatment. RNA quality was tested using Bioanalyzer 2100 (Agilent). Samples with RIN > 9.5 were sequenced using the Illumina HiSeq 2500, to a minimum of 30 million 50 bp paired-end reads per sample. Reads were aligned with TopHat 2.1.1 to the human Ensembl cDNA build, and subsequently counted and normalized using Cufflinks 2.2.1. Two repeats of each of the two cell lines were processed independently and the expression values averaged over transcriptomes. The data have been deposited in NCBI's Gene Expression Omnibus and are accessible through GEO Series accession number GSE131753 (<https://www.ncbi.nlm.nih.gov/geo/query/acc.cgi?acc=GSE131753>).

### Animals

All studies on mice were approved by the Cincinnati Children's Medical Center Animal Care and Use Committee (CCHMC IACUC 2017-0051) and comply with the National Institutes of Health guidelines. All studies were carried out on FVB/N background mice. Mice were housed in plastic cages with ad libitum diet and 10-h dark/14-h light cycle.

### Mouse Tissue Collection

Female FVB/N mice aged 8–10 weeks were mated with male FVB/N mice from 8 PM until 8 AM, and subsequently separated. Female mice were checked for vaginal plug (E 0.5). For each time point, tissues from three dams were collected. From E13.5 to E18.5, tissues were collected at 8 AM; for E19.0, tissues were collected at 8 PM. Fetal membranes and placenta were collected from two fetuses of each dam. The placenta was then manually separated into the labyrinth part and the junctional zone and decidual part. On E15.5, uterus and ovary were collected for each dam; fetal brain, limb, liver, and lung tissues were collected from two fetuses of each dam. Uterus and ovary tissue were also collected from three virgin female mice. Testis was collected from six males. Other adult tissues, including brain, kidney, liver, lung, muscle, and spleen were each collected from six mice (three males and three females).

For mouse preimplantation embryo collection, 3-week-old female FVB/N mice were treated with pregnant mare serum gonadotropin (Prospec PMSG) 5 IU/mouse through peritoneal injection at 12 PM. About 47 h after PMSG injection (11

AM), mice were treated with hCG (Millipore 230734) 5 IU/mouse through peritoneal injection, then mated with male FVB/N mice. Female mice were separated from male at 8 AM next morning, and vagina plug was checked at that time. About 42–44 h, 68–70 h, and 98–100 h after hCG injection, 2-cell stage embryos, 8-cell stage embryos, and blastocyst were collected, respectively. Embryos from the same female were combined for total RNA collection.

### Total RNA Isolation and Quantitative PCR

Total RNA from ovary and preimplantation embryos was isolated using RNeasy plus micro kit (Qiagen). Total RNA from all other tissues and cells was isolated using EZ tissue/cell total RNA miniprep kit (EZ BioResearch). RNA was reverse transcribed to cDNA using the QuantiTect Reverse Transcriptase Kit (Qiagen). Quantitative PCR (qPCR) for human term placenta and fetal membrane samples and BeWo cell differentiation was performed using EXPRESS SYBR GreenER (ThermoFisher Scientific). All other qPCRs were performed using TaqMan Fast Advanced Master Mix and pre-designed TaqMan gene expression assay (ThermoFisher Scientific). All qPCR reactions were run on Applied Biosystems StepOnePlus Real-Time PCR instrument. Species-specific *GPDH* is used as endogenous control.

### RNAscope In Situ Assay of Mouse Implantation Site

On E15.5 implantation site samples (placentas with attached fetal membranes and uterus wall) were collected as described earlier. Samples were fixed in 10% neutral buffered formalin for 24 h at room temperature, washed with PBS, dehydrated in standard ethanol series followed by embedding in paraffin. Paraffin blocks were cut into 5  $\mu$ m sections using a microtome. RNAscope assay was carried out using RNAscope 2.5 HD Duplex kit (Cat No. 322430). Probe-Mm-Trim1-E4-E6-C2 (Cat No. 478441-C2) and Probe-Mm-Trim2-E5-E7 (Cat No. 473731) were used to detect the target genes. 2-plex Negative Control Probe (Cat. No. 320751) was used to evaluate non-specific signals.

### Statistical Analysis

All statistical analysis was performed in RStudio version 1.1.383. Specific statistical tests are described earlier.

### Supplementary Material

Supplementary data are available at *Molecular Biology and Evolution* online.

### Acknowledgments

The authors would like to thank Dr Günter Wagner for commenting on earlier versions of the article. This work was supported by the March of Dimes Prematurity Research Center Ohio Collaborative, and the National Institutes of Health/Eunice Kennedy Shriver National Institute of Child Health and Human Development (grant number 5R01HD091527).

### Author Contributions

X.Z., H.N.J., and L.J.M. conceived the project. X.Z. and M.P. performed research and analyzed the data. X.Z. wrote the original draft and all other authors reviewed and edited the article.

### References

- Aldo PB, Mulla MJ, Romero R, Mor G, Abrahams VM. 2010. Viral ssRNA induces first trimester trophoblast apoptosis through an inflammatory mechanism. *Am J Reprod Immunol.* 64(1):27–37.
- Armstrong DL, McGowen MR, Weckle A, Pantham P, Caravas J, Agnew D, Benirschke K, Savage-Rumbaugh S, Nevo E, Kim CJ, et al. 2017. The core transcriptome of mammalian placentas and the divergence of expression with placental shape. *Placenta* 57:71–78.
- Basak S, Dubanchet S, Zourbas S, Chaouat G, Das C. 2002. Expression of proinflammatory cytokines in mouse blastocysts during implantation: modulation by steroid hormones. *Am J Reprod Immunol.* 47(1):2–11.
- Bell JL, Malyukova A, Holien JK, Koach J, Parker MW, Kavallaris M, Marshall GM, Cheung BB. 2012. TRIM16 acts as an E3 ubiquitin ligase and can heterodimerize with other TRIM family members. *PLoS One* 7(5):e37470.
- Bharaj P, Atkins C, Luthra P, Giraldo MI, Dawes BE, Miorin L, Johnson JR, Krogan NJ, Basler CF, Freiberg AN, et al. 2017. The host E3-ubiquitin ligase TRIM6 ubiquitinates the ebola virus VP35 protein and promotes virus replication. *J Virol.* 91(18):e00833-17.
- Calleja-Agius J, Jauniaux E, Pizzey AR, Muttukrishna S. 2012. Investigation of systemic inflammatory response in first trimester pregnancy failure. *Hum Reprod.* 27(2):349–357.
- Cao T, Borden KL, Freemont PS, Etkin LD. 1997. Involvement of the rfp tripartite motif in protein-protein interactions and subcellular distribution. *J Cell Sci.* 110 (Pt 14):1563–1571.
- Capellini I. 2012. The evolutionary significance of placental interdigitation in mammalian reproduction: contributions from comparative studies. *Placenta* 33(10):763–768.
- Capra JA, Stolzer M, Durand D, Pollard KS. 2013. How old is my gene? *Trends Genet.* 29(11):659–668.
- Carthagen L, Bergamaschi A, Luna JM, David A, Uchil PD, Margottin-Goguet F, Mothes W, Hazan U, Transy C, Pancino G, et al. 2009. Human TRIM gene expression in response to interferons. *PLoS One* 4(3):e4894.
- Castresana J. 2000. Selection of conserved blocks from multiple alignments for their use in phylogenetic analysis. *Mol Biol Evol.* 17(4):540–552.
- Chaouat G. 2013. Inflammation, NK cells and implantation: friend and foe (the good, the bad and the ugly?): replacing placental viviparity in an evolutionary perspective. *J Reprod Immunol.* 97(1):2–13.
- Chavan AR, Bhullar BA, Wagner GP. 2016. What was the ancestral function of decidual stromal cells? A model for the evolution of eutherian pregnancy. *Placenta* 40:40–51.
- Chavan AR, Griffith OW, Wagner GP. 2017. The inflammation paradox in the evolution of mammalian pregnancy: turning a foe into a friend. *Curr Opin Genet Dev.* 47:24–32.
- Chen J, Swofford R, Johnson J, Cummings BB, Rogel N, Lindblad-Toh K, Haerty W, Palma FD, Regev A. 2019. A quantitative framework for characterizing the evolutionary history of mammalian gene expression. *Genome Res.* 29(1):53–63.
- Chuong EB. 2013. Retroviruses facilitate the rapid evolution of the mammalian placenta. *Bioessays* 35(10):853–861.
- Chuong EB, Rumi MA, Soares MJ, Baker JC. 2013. Endogenous retroviruses function as species-specific enhancer elements in the placenta. *Nat Genet.* 45(3):325–329.
- Coan PM, Ferguson-Smith AC, Burton GJ. 2005. Ultrastructural changes in the interhaemal membrane and junctional zone of the murine chorioallantoic placenta across gestation. *J Anat.* 207(6):783–796.

- Denton JF, Lugo-Martinez J, Tucker AE, Schrider DR, Warren WC, Hahn MW, 2014. Extensive error in the number of genes inferred from draft genome assemblies. *PLoS Comput Biol.* 10(12):e1003998.
- Elliot MG, Crespi BJ, 2006. Placental invasiveness mediates the evolution of hybrid inviability in mammals. *Am Nat.* 168(1):114–120.
- Elliot MG, Crespi BJ, 2009. Phylogenetic evidence for early hemochorial placentation in Eutheria. *Placenta* 30(11):949–967.
- Fagerberg L, Hallström BM, Oksvold P, Kampf C, Djureinovic D, Odeberg J, Habuka M, Tahmasebpoor S, Danielsson A, Edlund K, et al. 2014. Analysis of the human tissue-specific expression by genome-wide integration of transcriptomics and antibody-based proteomics. *Mol Cell Proteomics.* 13(2):397–406.
- Ferretti C, Bruni L, Dangles-Marie V, Pecking AP, Bellet D, 2006. Molecular circuits shared by placental and cancer cells, and their implications in the proliferative, invasive and migratory capacities of trophoblasts. *Hum Reprod Update.* 13(2):121–141.
- Frankenberg S, 2018. Pre-gastrula development of non-eutherian mammals. *Curr Top Dev Biol.* 128:237–266.
- Frankenberg S, Renfree MB, 2018. Conceptus coats of marsupials and monotremes. *Curr Top Dev Biol.* 130:357–377.
- Ganser-Pornillos BK, Chandrasekaran V, Pornillos O, Sodroski JG, Sundquist WI, Yeager M, 2011. Hexagonal assembly of a restricting TRIM5alpha protein. *Proc Natl Acad Sci U S A.* 108(2):534–539.
- Garratt M, Gaillard JM, Brooks RC, Lemaître JF, 2013. Diversification of the eutherian placenta is associated with changes in the pace of life. *Proc Natl Acad Sci U S A.* 110(19):7760–7765.
- Gopinathan G, Milagre C, Pearce OM, Reynolds LE, Hodiola-Dilke K, Leinster DA, Zhong H, Hollingsworth RE, Thompson R, Whiteford JR, et al. 2015. Interleukin-6 stimulates defective angiogenesis. *Cancer Res.* 75(15):3098–3107.
- Griffith OW, Chavan AR, Protopapas S, Maziarz J, Romero R, Wagner GP, 2017. Embryo implantation evolved from an ancestral inflammatory attachment reaction. *Proc Natl Acad Sci U S A.* 114(32):E6566–E6575.
- Gu F, Wang C, Wei F, Wang Y, Zhu Q, Ding L, Xu W, Zhu C, Cai C, Qian Z, et al. 2018. STAT6 degradation and ubiquitinated TRIML2 are essential for activation of human oncogenic herpesvirus. *PLoS Pathog.* 14(12):e1007416.
- Haig D, 2012. Retroviruses and the placenta. *Curr Biol.* 22(15):R609–R613.
- Hayashi F, Kasamatsu A, Endo-Sakamoto Y, Eizuka K, Hiroshima K, Kita A, Saito T, Koike K, Tanzawa H, Uzawa K, 2019. Increased expression of tripartite motif (TRIM) like 2 promotes tumoral growth in human oral cancer. *Biochem Biophys Res Commun.* 508(4):1133–1138.
- Hunt BG, Ometto L, Wurm Y, Shoemaker D, Yi SV, Keller L, Goodisman MA, 2011. Relaxed selection is a precursor to the evolution of phenotypic plasticity. *Proc Natl Acad Sci U S A.* 108(38):15936–15941.
- Hurst LD, Smith NG, 1999. Do essential genes evolve slowly? *Curr Biol.* 9(14):747–750.
- Ibrahim MM, Karabacak A, Glihs A, Kolundzic E, Hirsekorn A, Carda A, Tursun B, Zinzen RP, Lacadie SA, Ohler U, 2018. Determinants of promoter and enhancer transcription directionality in metazoans. *Nat Commun.* 9(1):4472.
- Imakawa K, Nakagawa S, 2017. The phylogeny of placental evolution through dynamic integrations of retrotransposons. *Prog Mol Biol Transl Sci.* 145:89–109.
- Jablonska J, Leschner S, Westphal K, Lienenklaus S, Weiss S, 2010. Neutrophils responsive to endogenous IFN-beta regulate tumor angiogenesis and growth in a mouse tumor model. *J Clin Invest.* 120(4):1151–1164.
- James LC, Keeble AH, Khan Z, Rhodes DA, Trowsdale J, 2007. Structural basis for PRYSPRY-mediated tripartite motif (TRIM) protein function. *Proc Natl Acad Sci U S A.* 104(15):6200–6205.
- Johnson MR, Riddle AF, Grudzinskas JG, Sharma V, Collins WP, Nicolaides KH, 1993. The role of trophoblast dysfunction in the aetiology of miscarriage. *Br J Obstet Gynaecol.* 100(4):353–359.
- Kang HJ, Rosenwaks Z, 2018. p53 and reproduction. *Fertil Steril.* 109(1):39–43.
- Kumar S, Stecher G, Li M, Knyaz C, Tamura K, 2018. MEGA X: molecular evolutionary genetics analysis across computing platforms. *Mol Biol Evol.* 35(6):1547–1549.
- Kumar S, Stecher G, Suleski M, Hedges SB, 2017. TimeTree: a resource for timelines, timetrees, and divergence times. *Mol Biol Evol.* 34(7):1812–1819.
- Kung CP, Khaku S, Jennis M, Zhou Y, Murphy ME, 2015. Identification of TRIML2, a novel p53 target, that enhances p53 SUMOylation and regulates the transactivation of proapoptotic genes. *Mol Cancer Res.* 13(2):250–262.
- Lek M, Karczewski KJ, Minikel EV, Samocha KE, Banks E, Fennell T, O'Donnell-Luria AH, Ware JS, Hill AJ, Cummings BB, et al. 2016. Analysis of protein-coding genetic variation in 60,706 humans. *Nature* 536(7616):285–291.
- Luckett WP, 1975. The development of primordial and definitive amniotic cavities in early Rhesus monkey and human embryos. *Am J Anat.* 144(2):149–167.
- Lupas A, Van Dyke M, Stock J, 1991. Predicting coiled coils from protein sequences. *Science* 252(5009):1162–1164.
- Marchand M, Horcajadas JA, Esteban FJ, McElroy SL, Fisher SJ, Giudice LC, 2011. Transcriptomic signature of trophoblast differentiation in a human embryonic stem cell model. *Biol Reprod.* 84(6):1258–1271.
- Marchler-Bauer A, Derbyshire MK, Gonzales NR, Lu S, Chitsaz F, Geer LY, Geer RC, He J, Gwadz M, Hurwitz DI, et al. 2015. CDD: NCBI's conserved domain database. *Nucleic Acids Res.* 43(D1):D222–D226.
- Marin R, Cortez D, Lamanna F, Pradeepa MM, Leushkin E, Julien P, Liechti A, Halbert J, Brüning T, Mössinger K, et al. 2017. Convergent origination of a Drosophila-like dosage compensation mechanism in a reptile lineage. *Genome Res.* 27(12):1974–1987.
- Mikhaylichenko O, Bondarenko V, Harnett D, Schor IE, Males M, Viales RR, Furlong E, 2018. The degree of enhancer or promoter activity is reflected by the levels and directionality of eRNA transcription. *Genes Dev.* 32(1):42–57.
- Mor G, 2008. Inflammation and pregnancy: the role of toll-like receptors in trophoblast-immune interaction. *Ann N Y Acad Sci.* 1127(1):121–128.
- Mor G, Cardenas I, 2010. The immune system in pregnancy: a unique complexity. *Am J Reprod Immunol.* 63(6):425–433.
- Moreno-Hagelsieb G, Latimer K, 2008. Choosing BLAST options for better detection of orthologs as reciprocal best hits. *Bioinformatics* 24(3):319–324.
- Muroi Y, Sakurai T, Hanashi A, Kubota K, Nagaoka K, Imakawa K, 2009. CD9 regulates transcription factor GCM1 and ERVWE1 expression through the cAMP/protein kinase A signaling pathway. *Reproduction* 138(6):945–951.
- Necsulea A, Soumillon M, Warnefors M, Liechti A, Daish T, Zeller U, Baker JC, Grützner F, Kaessmann H, 2014. The evolution of lncRNA repertoires and expression patterns in tetrapods. *Nature* 505(7485):635–640.
- O'Leary MA, Bloch JJ, Flynn JJ, Gaudin TJ, Giallombardo A, Giannini NP, Goldberg SL, Kraatz BP, Luo ZX, Meng J, et al. 2013. The placental mammal ancestor and the post-K-Pg radiation of placentals. *Science* 339(6120):662–667.
- Ozato K, Shin DM, Chang TH, Morse HC III, 2008. TRIM family proteins and their emerging roles in innate immunity. *Nat Rev Immunol.* 8(11):849–860.
- Palchetti S, Starace D, De Cesaris P, Filippini A, Ziparo E, Riccioli A, 2015. Transfected poly(I:C) activates different dsRNA receptors, leading to apoptosis or immunoadjuvant response in androgen-independent prostate cancer cells. *J Biol Chem.* 290(9):5470–5483.
- Pijnenborg R, Robertson WB, Brosens I, Dixon G, 1981. Review article: trophoblast invasion and the establishment of haemochorial placentation in man and laboratory animals. *Placenta* 2(1):71–91.
- Quintero-Cadena P, Sternberg PW, 2016. Enhancer sharing promotes neighborhoods of transcriptional regulation across eukaryotes. *G3 (Bethesda)* 6(12):4167–4174.
- Renfree MB, 2010. Review: marsupials: placental mammals with a difference. *Placenta* 31(Suppl):S21–S26.
- Ronquist F, Huelsenbeck JP, 2003. MrBayes 3: Bayesian phylogenetic inference under mixed models. *Bioinformatics* 19(12):1572–1574.

- Sanchez JG, Okreglicka K, Chandrasekaran V, Welker JM, Sundquist WI, Pornillos O, 2014. The tripartite motif coiled-coil is an elongated antiparallel hairpin dimer. *Proc Natl Acad Sci U S A.* 111(7):2494–2499.
- Sardiello M, Cairo S, Fontanella B, Ballabio A, Meroni G, 2008. Genomic analysis of the TRIM family reveals two groups of genes with distinct evolutionary properties. *BMC Evol Biol.* 8(1):225.
- Scotland KB, Chen S, Sylvester R, Gudas LJ, 2009. Analysis of Rex1 (zfp42) function in embryonic stem cell differentiation. *Dev Dyn.* 238(8):1863–1877.
- Si Z, Vandegraaff N, O’Huigin C, Song B, Yuan W, Xu C, Perron M, Li X, Marasco WA, Engelman A, et al. 2006. Evolution of a cytoplasmic tripartite motif (TRIM) protein in cows that restricts retroviral infection. *Proc Natl Acad Sci U S A.* 103(19):7454–7459.
- Tekaia F, 2016. Inferring orthologs: open questions and perspectives. *Genomics Insights* 9:17–28.
- Versteeg GA, Benke S, García-Sastre A, Rajsbaum R, 2014. InTRIMsic immunity: positive and negative regulation of immune signaling by tripartite motif proteins. *Cytokine Growth Factor Rev.* 25(5):563–576.
- Versteeg GA, Rajsbaum R, Sánchez-Aparicio MT, Maestre AM, Valdiviezo J, Shi M, Inn KS, Fernandez-Sesma A, Jung J, García-Sastre A, 2013. The E3-ligase TRIM family of proteins regulates signaling pathways triggered by innate immune pattern-recognition receptors. *Immunity* 38(2):384–398.
- Wang X, Douglas KC, Vandeberg JL, Clark AG, Samollow PB, 2014. Chromosome-wide profiling of X-chromosome inactivation and epigenetic states in fetal brain and placenta of the opossum, *Monodelphis domestica*. *Genome Res.* 24(1):70–83.
- Wang X, Gorospe M, Huang Y, Holbrook NJ, 1997. p27Kip1 overexpression causes apoptotic death of mammalian cells. *Oncogene* 15(24):2991–2997.
- Wildman DE, Chen C, Erez O, Grossman LI, Goodman M, Romero R, 2006. Evolution of the mammalian placenta revealed by phylogenetic analysis. *Proc Natl Acad Sci U S A.* 103(9):3203–3208.
- Worobey M, Bjork A, Wertheim JO, 2007. Point, counterpoint: the evolution of pathogenic viruses and their human hosts. *Annu Rev Ecol Evol Syst.* 38(1):515–540.
- Xie H, Sun X, Piao Y, Jegga AG, Handwerker S, Ko MS, Dey SK, 2012. Silencing or amplification of endocannabinoid signaling in blastocysts via CB1 compromises trophoblast cell migration. *J Biol Chem.* 287(38):32288–32297.
- Yang Z, 2007. PAML 4: phylogenetic analysis by maximum likelihood. *Mol Biol Evol.* 24(8):1586–1591.
- Yue F, Cheng Y, Breschi A, Vierstra J, Wu W, Ryba T, Sandstrom R, Ma Z, Davis C, Pope BD, et al. 2014. A comparative encyclopedia of DNA elements in the mouse genome. *Nature* 515(7527):355–364.
- Zenclussen AC, Blois S, Stumpo R, Olmos S, Arias K, Malan Borel I, Roux ME, Margni RA, 2003. Murine abortion is associated with enhanced interleukin-6 levels at the fetomaternal interface. *Cytokine* 24(4):150–160.
- Zenclussen AC, Kortebani G, Mazzolli A, Margni R, Malan Borel I, 2000. Interleukin-6 and soluble interleukin-6 receptor serum levels in recurrent spontaneous abortion women immunized with paternal white cells. *Am J Reprod Immunol.* 44(1):22–29.
- Zhang JY, Zhou Q, 2019. On the regulatory evolution of new genes throughout their life history. *Mol Biol Evol.* 36(1):15–27.
- Zhu D, Gong X, Miao L, Fang J, Zhang J, 2017. Efficient induction of syncytiotrophoblast layer II cells from trophoblast stem cells by canonical Wnt signaling activation. *Stem Cell Rep.* 9(6):2034–2049.